

Insights into the Milky Way pulsar–black hole population using radio and gravitational wave observations

NIHAN POL,¹ MAURA MCLAUGHLIN,^{2,3} AND DUNCAN R. LORIMER^{2,3}

¹*Department of Physics and Astronomy, Vanderbilt University, 2301 Vanderbilt Place, Nashville, TN 37235, USA*

²*Department of Physics and Astronomy, West Virginia University, Morgantown, WV 26506-6315*

³*Center for Gravitational Waves and Cosmology, West Virginia University, Chestnut Ridge Research Building, Morgantown, West Virginia 26505*

ABSTRACT

The detection of two NS–BH mergers by LIGO–Virgo provided the first direct confirmation of the existence of this type of system in the Universe. These detections also imply the existence of pulsar–black hole systems. In this analysis, we use the non-detection of any PSR–BH systems in current radio surveys to estimate a 95% upper limit of ~ 150 PSR–BH binary systems that are beaming towards the Earth in the Milky Way. This corresponds to a 95% upper limit of $\mathcal{R}_{\text{LIGO}} = 7.6 \text{ yr}^{-1}$ on the merger detection rate for the LIGO–Virgo network scaled to a range distance of 100 Mpc, which is consistent with the rates derived by LIGO–Virgo. In addition, for the first time, we use the merger detection rates estimate by LIGO–Virgo to predict the number of detectable PSR–BH systems in the Milky Way. We find there to be $\langle N_{\text{obs,NSBH,e}} \rangle = 2_{-1}^{+5}$ and $\langle N_{\text{obs,NSBH,p}} \rangle = 6_{-4}^{+7}$ detectable PSR–BH systems in the Milky Way corresponding to the event-based and population-based merger detection rates estimated by LIGO–Virgo respectively. We estimate the probability of detecting these PSR–BH systems with current radio pulsar surveys, showing that the Arecibo PALFA survey has the highest probability of detecting a PSR–BH system, while surveys with recently commissioned and planned telescopes are almost guaranteed to detect one of these systems. Finally, we discuss the hurdles in detecting PSR–BH systems and how these can be overcome in the future.

Keywords: pulsars: general — pulsars: binary — gravitational waves

1. INTRODUCTION

Since their discovery more than 50 years ago, pulsars, which are rotating neutron stars (NSs), have been observed in binaries around main sequence stars, white dwarf stars, and other neutron stars (Lorimer 2005). To date, we have detected more than 300 binary pulsar systems (from the ATNF pulsar catalog, Manchester et al. 2005), which include systems such as a double neutron star system with both neutron stars observed as pulsars (Lyne et al. 2004; Burgay et al. 2005) and a triple system with a pulsar in an orbit consisting of two other white dwarf companions (Ransom et al. 2014). These systems have allowed tests of general relativity in the strong-field regime (Kramer et al. 2006), constraints on alternative theories of gravity (for e.g., Kramer & Wex 2009; Ransom et al. 2014), insights into magnetospheric physics (for e.g., Breton et al. 2012; Lomiashvili & Lyutikov 2014), as well as constraints on different stellar evolution models (for e.g., Stairs 2004; Ferdman et al. 2020). However, despite this diversity in the binary pul-

sar systems discovered to date, there has been no confirmed detection of a neutron star– or pulsar–black hole (PSR–BH) system.

The LIGO–Virgo collaboration recently reported the detection of two NS–BH mergers (Abbott et al. 2021). These detections conclusively established the existence of this type of system in the (local) Universe, with the mass of the neutron stars and black holes in the two detections falling between 90% credible bounds of $1.2 M_{\odot}$ and $2.2 M_{\odot}$ and $3.6 M_{\odot}$ and $10.1 M_{\odot}$, respectively. The merger rate density based on these two detections was estimated to be $\mathcal{R} = 45_{-33}^{+75} \text{ Gpc}^{-3} \text{ yr}^{-1}$, which when scaled to a range distance of $D_r = 100 \text{ Mpc}$, results in a merger detection rate of $\mathcal{R}_{\text{event}} = 0.19_{-0.14}^{+0.31} \text{ yr}^{-1}$ (Abbott et al. 2021), with the errors representing the 90% credible region. However, as described in Abbott et al. (2021), if a broader range of priors is assumed for the NS–BH mergers, the corresponding merger rate density is slightly higher at $\mathcal{R} = 130_{-69}^{+112} \text{ Gpc}^{-3} \text{ yr}^{-1}$,

which scaled to a range distance of 100 Mpc results in a merger detection rate of $\mathcal{R}_{\text{pop}} = 0.54_{-0.28}^{+0.47} \text{ yr}^{-1}$.

Based on these merger rate estimates, [Abbott et al. \(2021\)](#) found that formation mechanisms such as isolated binary evolution (for e.g., [Belczynski et al. 2016, 2002](#); [Broekgaarden et al. 2021](#)), in young stellar clusters (for e.g., [Santoliquido et al. 2020](#)), and in disks of active galactic nuclei ([McKernan et al. 2020](#)) all produce merger rate estimates that are consistent with those derived using the observed NS–BH mergers. In the consideration of NS–BH or PSR–BH systems in the Milky Way, the formation channel involving active galactic nuclei disks is not applicable, while the rate predictions from young stellar clusters, ranging between $0.1\text{--}100 \text{ Gpc}^{-3} \text{ yr}^{-1}$ are in slight tension with the larger, population based rate estimate from [Abbott et al. \(2021\)](#). This leaves the isolated binary formation channel as the most viable formation mechanism for NS–BH or PSR–BH systems. Additionally, dynamical formation scenarios ([Portegies Zwart & McMillan 2000](#)) produce merger rates that are inconsistent with the observed merger rate, unless special accommodations are made in the stellar evolution processes (for e.g., [Ye et al. 2020](#); [Clausen et al. 2013](#)).

Given these different formation channels for NS–BH and PSR–BH systems, many radio surveys have been designed and executed over multiple decades to target each of these formation channels. Finding PSR–BH systems has been a major objective for all of the large radio pulsar surveys that have been carried out to date (for e.g., [Cordes et al. 2006](#); [Foster et al. 1995](#); [Manchester et al. 2001](#); [Stovall et al. 2014](#); [Keith et al. 2010](#)), whose primary focus is searching along the plane of the Galaxy for systems formed through the isolated binary channel. There have also been a number of targeted radio pulsar surveys of globular and open clusters in the Milky Way ([Urquhart et al. 2020](#); [Ridolfi et al. 2021](#); [Pan et al. 2021](#)), as well as the Galactic center ([Rajwade et al. 2017](#); [Hyman et al. 2019](#); [Eatough et al. 2013](#)), which aim to detect systems formed through both the isolated binary and dynamical formation channels. However, none of these surveys have reported a detection of a PSR–BH system.

While the two NS–BH merger detections made by LIGO–Virgo provided invaluable scientific results about stellar evolution, component masses and even tests of general relativity (GR, [Abbott et al. 2021](#)), detecting a PSR–BH system in the Milky Way stands to be just as valuable. A pulsar, as a regular rotator, can be used as a clock in orbit around the black hole in the PSR–BH system and timing observations of the pulsar will allow direct tests of the space-time surrounding the black hole,

as well as probing the properties of the black hole itself. For example, [Wex & Kopeikin \(1999\)](#) showed that detecting a PSR–BH system would allow us to measure the mass of the black hole to an accuracy better than $\sim 5\%$, while measurement of orbital precession can allow us to estimate the spin of the black hole. [Wex et al. \(2013\)](#) and [Liu et al. \(2014\)](#) showed that PSR–BH systems can be excellent sources to test the behaviour of GR in the strong-field regime, complementary to the tests that are possible with gravitational wave merger detections made by LIGO–Virgo. [Liu et al. \(2014\)](#) also showed that PSR–BH systems provide excellent tests of alternative theories of gravity, even if those theories predict black holes with identical properties to those predicted by GR.

Given the wealth of science offered by PSR–BH systems, it is worth aggregating the information available so far through radio surveys and gravitational wave observations to infer the size of the population and detection prospects for PSR–BH systems in the Galaxy. In [Sec. 2](#), we describe the process, and estimate and compare the NS–BH merger detection rate using the non-detection of PSR–BH systems in current radio surveys. In [Sec. 3](#), we develop and implement the methodology for using the merger detection rate estimated by gravitational wave observations of NS–BH mergers to estimate the Milky Way population of PSR–BH systems. In [Sec. 4](#) discuss the prospects for detecting these systems as well as hurdles involved in trying to find these systems. In [Sec. 5](#) we offer our conclusions.

2. RADIO SURVEY CONSTRAINTS ON PSR–BH POPULATION

2.1. PSR–BH population and survey parameters

We use the PSRPOPPY software package ([Bates et al. 2014](#)) to simulate the pulsar population and radio surveys in this analysis. Since we are modelling PSR–BH binaries, we model the corresponding degradation in the S/N ratio due to the orbital motion of the pulsar by using the neural network implementation of the orbital degradation factor ([Bagchi et al. 2013](#)) described in [Pol et al. \(2021\)](#).

The mass of the pulsars is assumed to follow the distribution given in [Özel & Freire \(2016\)](#) for canonical (long-period) pulsars and the mass of the companion is assumed to be uniform between $3 M_{\odot}$ and $100 M_{\odot}$ ([Chattopadhyay et al. 2021](#)). We assume that the inclination is uniform in $\sin(i)$, where the inclination angle, i , is allowed to vary between 0° and 90° , angle of periastron passage is uniform between 0° and 360° , and eccentricity uniform between 0 and 0.9. We allow the orbital period to vary between 10^{-3} days and 10 days, where the upper limit is chosen such that all systems

merge, on average, within a Hubble time. For the calculation of the orbital degradation factor, we use only the second harmonic, assuming that the pulsar is an orthogonal rotator and hence, most of its power is contained in the second harmonic (Pol et al. 2019, 2021).

Since most of the formation channels for PSR–BH binaries predict that the NS is born after the BH in the system (for e.g., Kruckow et al. 2018), the pulsar is unlikely to undergo any period of accretion from the companion, and will be a canonical pulsar. Thus, we assume the pulsar spin periods to have the same distribution as that for the canonical pulsar distribution, i.e. a log-normal distribution with $\langle \log_{10} P \rangle = 2.7$ and $\sigma_{\log_{10} P} = 0.34$ (Lorimer et al. 2006). We also assume a log-normal luminosity distribution with mean $\langle \log_{10} L \rangle = -1.1$ ($L = 0.07 \text{ mJy kpc}^2$) and standard deviation $\sigma_{\log_{10} L} = 0.9$ (Faucher-Giguère & Kaspi 2006). We also consider surveys at different radio frequencies, and thus assume a normal spectral index distribution with mean $\alpha = 1.4$ and standard deviation $\beta = 1$ (Bates et al. 2013). We assume the radial distribution of pulsars in the Galaxy to follow that from Lorimer et al. (2006), and the z -height distribution as described by a two-sided exponential with a scale height of $z_0 = 330 \text{ pc}$.

For canonical pulsars, the beaming fraction, F , which represents the percentage of the sky covered by a pulsar’s beam, can be related to the spin period (Tauris & Manchester 1998),

$$F = 9 \left(\log_{10} \frac{P}{10} \right)^2 + 3, \quad (1)$$

where P is the spin period of the pulsar in seconds. The beaming correction factor, $f_b = 100/F$, corrects for the number of systems whose emission beam does not cross the line-of-sight to Earth.

Finally, we need to know the distribution of the effective lifetime, τ_{life} , of the PSR–BH system. The effective lifetime is defined the amount of time for which the PSR–BH binary is detectable through the pulsar in the system. Thus, for the canonical pulsars in this analysis, $\tau_{\text{life}} = \tau_c + \min(\tau_{\text{death}}, \tau_{\text{merger}})$, where τ_c is the characteristic age of the pulsar, τ_{death} is the time after which the pulsar crosses into the so-called “death valley” (Chen & Ruderman 1993; Zhang 2003) and ceases to be radio-visible, and τ_{merger} is the time until the PSR–BH system merges through the emission of gravitational waves. Since we use the “snapshot” modelling method of PSR-POPPY in our analysis (Bates et al. 2014), we do not have knowledge of the spin period derivative of our simulated pulsars, preventing us from calculating the characteristic ages of the pulsars in our simulation. In addition, there is large uncertainty associated with when pulsars

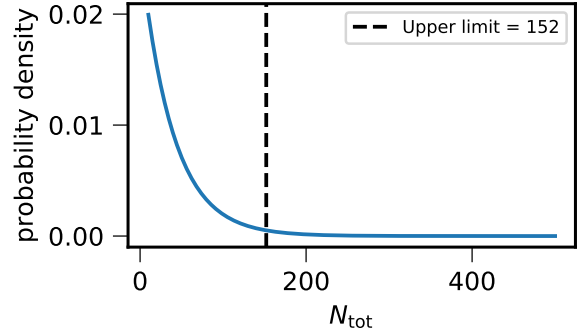


Figure 1. The 95% credible upper limit on the number of PSR–BH systems that are beaming towards the Earth given that none of the current radio surveys have detected one of these systems so far.

cross into the “death valley” (Zhang et al. 2000; Tan et al. 2018). Thus, for this analysis, we choose to adopt a log-uniform probability distribution for the effective lifetime of the PSR–BH systems in our simulations, with the binaries allowed to have lifetimes between 1 Myr and 1 Gyr.

The surveys that are used in our simulations are listed under “Current surveys” in Table 1. These surveys represent the largest radio pulsar surveys that have been carried out so far. We make the same assumption as in Pol et al. (2021), where we assume that these surveys will complete their design sky coverage. This, unfortunately, will not be possible for the surveys that were being carried out at the Arecibo radio telescope, namely the PALFA and AO327 surveys, due to its recent collapse, but we nevertheless assume that these surveys have covered $> 90\%$ of their designed sky coverage (Lazarus et al. 2015; Deneva et al. 2013).

2.2. Statistical framework

In this approach, we use the the statistical framework developed by Kim et al. (2003) and used most recently in Pol et al. (2021) and Grunthal et al. (2021), and we refer the reader to them for details about the framework.

Similar to Pol et al. (2021), since no PSR–BH systems have been detected, we set $N_{\text{obs}} = 0$ in our analysis. The corresponding 95% confidence upper limit on the number of PSR–BH systems that are beaming towards Earth, N_{tot} , is shown in Fig. 1.

We convert this to the corresponding prediction of the LIGO merger detection rate (Kim et al. 2003; Kopparapu et al. 2008) and derive a 95% confidence upper limit on the merger detection rate for LIGO of $\mathcal{R}_{\text{LIGO}} = 7.6 \text{ yr}^{-1}$. This merger detection rate is shown in Fig. 2, along with the merger detection rates derived

Table 1. This table lists the telescope and survey parameters for the large pulsar surveys that are considered in this work.

Survey	Gain, G (K/Jy)	Center Frequency, f_c (MHz)	Bandwidth, B (MHz)	System temperature, T_{sys} (K)	Integration time, t_{int} (s)
<i>Current Surveys</i>					
PALFA ^a	8.5	1374	300	25	268
PMSURV ^b	0.6	1374	288	25	2100
AO327 ^c	10	327	25	100	50
GBNCC ^d	2	350	100	46	120
HTRU–low ^e	0.6	1352	340	25	340
HTRU–mid ^f	0.6	1352	340	25	540
<i>Future Surveys</i>					
FAST GPPS ^g	16	1250	450	25	300
DSA-2000 Pulsar survey ^h	2	1300	1300	25	600
MeerKAT Pulsar Survey ⁱ	2.8	1284	776	18	600

^a Pulsar Arecibo L-band Feed Array, [Cordes et al. \(2006\)](#)

^b Parkes Multibeam SURvey, [Manchester et al. \(2001\)](#)

^c Arecibo DRIFT scan survey, [Foster et al. \(1995\)](#)

^d Green Bank North Celestial Cap Survey, [Stovall et al. \(2014\)](#)

^e High Time Resolution Universe low-latitude survey [Keith et al. \(2010\)](#)

^f High Time Resolution Universe mid-latitude survey [Keith et al. \(2010\)](#)

^g Five hundred meter Aperture Spherical Telescope ([Nan et al. 2011](#)) Galactic Plane Pulsar Survey, [Han et al. \(2021\)](#)

^h Deep Synoptic Array, [Hallinan et al. \(2019\)](#)

ⁱ [Bailes et al. \(2020\)](#)

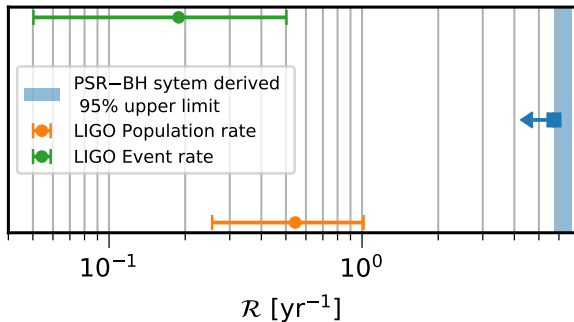


Figure 2. The 95% credible upper limit on the merger detection rate based on the non-detection of a PSR–BH system in current radio surveys is shown along with the merger detection rates derived using LIGO–Virgo detections of two merging NS–BH systems.

in [Abbott et al. \(2021\)](#). This merger detection rate is consistent with that derived by [Abbott et al. \(2021\)](#), which suggests that our assumption of no PSR–BH system detections in the Milky Way is compatible with the detection of two NS–BH mergers by LIGO–Virgo.

3. GRAVITATIONAL WAVE PREDICTION OF THE GALACTIC PSR–BH POPULATION

3.1. *Maximum likelihood Framework*

The statistical framework of [Kim et al. \(2003\)](#) assumes knowledge of the number of observed PSR–BH systems, N_{obs} , in order to derive upper limits on the size of the PSR–BH population and the corresponding merger rate. However, we can leave N_{obs} as a free parameter and use the merger rate estimated by [Abbott et al. \(2021\)](#) to place constraints on the number of observable PSR–BH systems in the Milky Way. Once we know the number of observable systems, we can follow the same process as in Sec. 2 to derive the size of the Milky Way PSR–BH population.

Following the same derivation as in [Kim et al. \(2003\)](#) but with N_{obs} as a free parameter and ignoring any normalization factors, the probability distribution for the size of the PSR–BH population can be written as,

$$P(N_{\text{tot}}) = \frac{\alpha^{N_{\text{obs}}+1} N_{\text{tot}}^{N_{\text{obs}}} e^{-\alpha N_{\text{tot}}}}{N_{\text{obs}}!}, \quad (2)$$

while the probability distribution for the merger rate,

$$P(\mathcal{R}) = \left[\frac{\alpha \tau_{\text{life}}}{f_b} \right]^{N_{\text{obs}}+1} \frac{\mathcal{R}^{N_{\text{obs}}} e^{-(\alpha \tau_{\text{life}}/f_b)\mathcal{R}}}{N_{\text{obs}}!}. \quad (3)$$

In addition to N_{obs} , the lifetime, τ_{life} , and the beaming correction factor, f_b , of the PSR–BH systems are also free parameters in Eq. 3. However, these two parameters are fully covariant with each other due to the structure of Eq. 3. As a result, we choose to model the ratio of these parameters, $\beta = f_b/\tau_{\text{life}}$, rather than the individual parameters themselves. Note that α can be considered as a constant in Eq. 3 since it depends primarily on the surveys used to search for the PSR–BH systems.

We use a non-linear maximum likelihood approach to find the values of N_{obs} and β . The residual function is defined as the difference between the probability density obtained from Eq. 3 (appropriately normalized) and the probability density function derived using LIGO’s observation of NS–BH mergers (Abbott et al. 2021). The non-linear optimization is performed using LMFIT (Newville et al. 2021), which is a Python package providing a high-level interface for optimization methods. LMFIT converts the residual function defined above into the corresponding χ^2 distribution by calculating the sum of the squares of the residual function values. We use the Levenberg-Marquardt (Moré 1978) method for minimizing this χ^2 distribution. Since LMFIT allows setting bounds on the parameters in Eq. 3, we constrain N_{obs} to the range [0, 100], and constrain β to the range [1×10^{-3} , 10]. The bounds on β were chosen such that they correspond to bounds of [1, 10] and [1 Myr, 1 Gyr] on f_b and τ_{life} respectively. Once the maximum likelihood solution is found, we explore the parameter space around the maximum likelihood solution using the EMCEE (Foreman-Mackey et al. 2013) sampler provided in LMFIT, thereby calculating the 95% credible regions around the maximum likelihood solution.

3.2. Testing the framework

To test this method, we first deploy it on the merging double neutron star (DNS) population in the Galaxy. There have been several recent studies that used the observed population of DNS systems in the Galaxy to predict the DNS merger detection rate for LIGO (e.g., Pol et al. 2019; Grunthal et al. 2021). We use the DNS merger detection rate estimate from Grunthal et al. (2021) as our target function in the non-linear optimization method described above. We can then judge the performance of our method by comparing the predicted value of N_{obs} with the real, known value of the number of merging DNS systems that have been observed so far (nine).

To derive α for the DNS population, we use the same process as described in Sec. 2.2. The DNS population properties are mostly similar to those described in Sec. 2.1 with some key differences. The mass of the secondary (and primary) is assumed to follow the distribution of DNS systems given in Özel & Freire (2016). The majority of pulsars in DNS systems have been observed as millisecond pulsars, but due to the dearth of these systems, the underlying period distribution is still unknown. Thus, we assume a uniform distribution of spin periods, ranging from 1 ms to 100 ms. Similarly, we assume a uniform distribution of orbital periods to correspond to the observed DNS systems (see Table 1 in Pol et al. 2019). The other population properties are the same as described in Sec. 2.1.

With this simulation setup, we calculate α_{DNS} , which is then used with the framework described in Sec. 3.1. To obtain the target merger detection rate distribution, we use the Galactic merger rate of $\mathcal{R} = 32_{-9}^{+19} \text{ Myr}^{-1}$ (Grunthal et al. 2021) and convert it to the LIGO merger detection rate, scaled to a range distance of 100 Mpc (Kopparapu et al. 2008). This merger detection rate, along with the best fit curve obtained from our optimization method is shown in Fig. 3. The maximum likelihood values thus obtained are $N_{\text{obs,DNS}} = 10.3 \pm 0.23$ and $\beta = 0.0404 \pm 0.0008$.

The corner plot showing the posterior distribution of these parameters and the distribution of $\langle N_{\text{obs}} \rangle$ (Eq. 7 in Kim et al. 2003) is also shown in Fig. 3. The recovered distribution of $\langle N_{\text{obs}} \rangle = 10_{-4}^{+8}$ is consistent with the nine observed DNS systems in the Galaxy. Additionally, even though we cannot set independent constraints on f_b or τ_{life} , we can use the knowledge of f_b for the observed DNS systems from Grunthal et al. (2021) to estimate the average lifetime of the Galactic DNS population using the maximum likelihood value of β . As shown in Pol et al. (2019) and Grunthal et al. (2021), there is a small group of DNS systems in the Galaxy that dominate the calculation of the merger detection rate. Using the average beaming correction factor of just these systems (Table 2 in Grunthal et al. 2021), $f_{b,\text{avg}} = 4.5$, we get the corresponding average lifetime of $\tau_{\text{life,avg}} = 111.4 \pm 0.3 \text{ Myr}$. This estimate is close to the average lifetime of 129 Myr for the group of DNS systems that contribute most to the merger detection rate.

This test shows that the optimization method presented in Sec. 3.1 can accurately predict the number of observable binary pulsar systems, as well as provide reasonable estimates of the average lifetime of the population under consideration given some knowledge of the beaming correction factor.

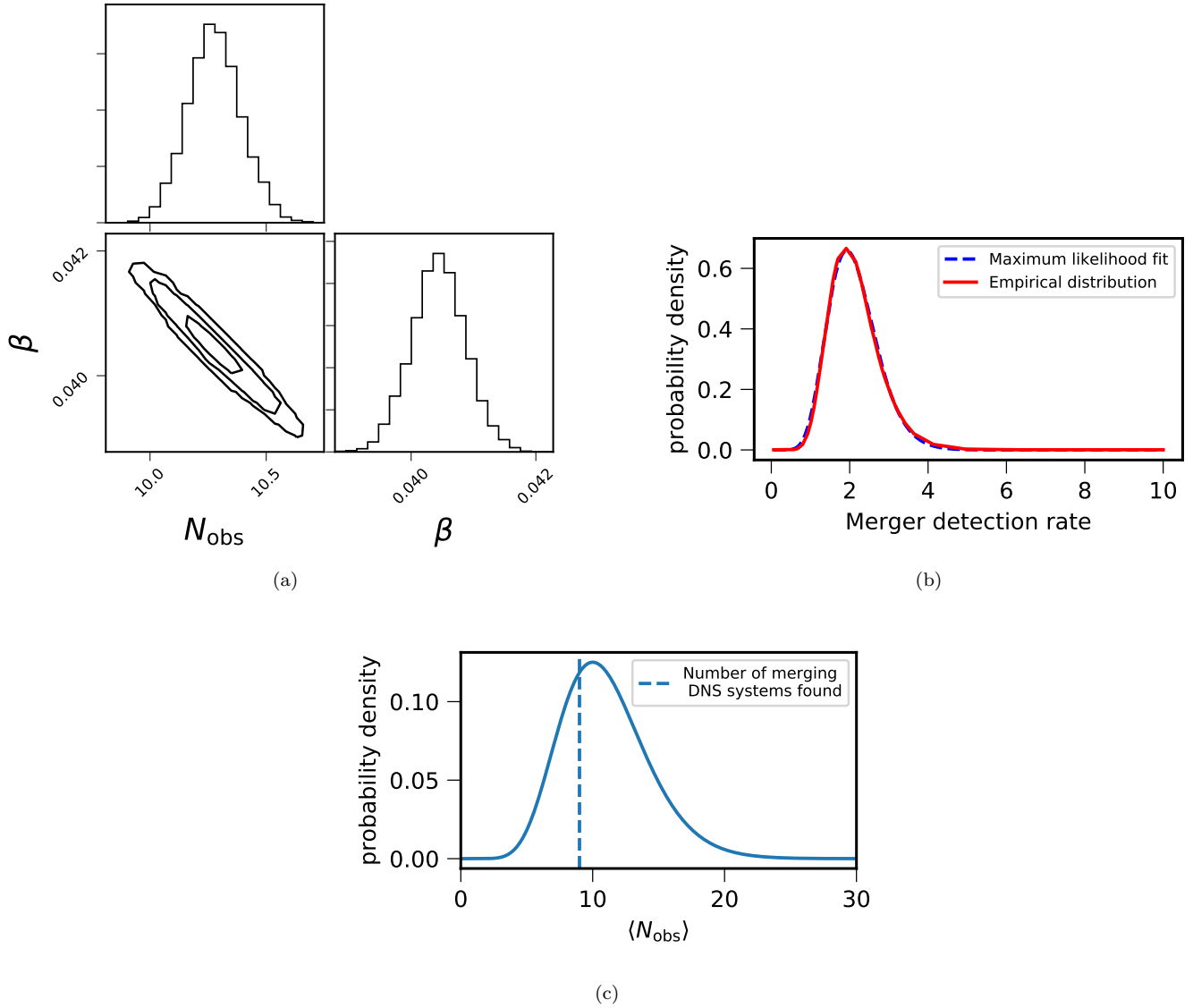


Figure 3. Results from the maximum likelihood analysis for the population of merging DNS systems in the Galaxy. (a): The posterior distribution on the parameters in Eq. 3. The contours represent the 1-, 2-, and 3- σ confidence intervals. (b): The probability distribution generated using the maximum likelihood parameters shown in panel (a) is compared with the empirical distribution derived in Grunthal et al. (2021) showing excellent agreement between the two distributions. (c): Distribution of the expected number of observable DNS systems from the maximum likelihood analysis described in Sec. 3.1. The vertical dashed line shows the number of DNS systems that will merge within a Hubble time that have been discovered in radio surveys so far (nine).

3.3. Estimating the number of observable PSR–BH systems in the Galaxy

Given the verification of the maximum likelihood framework in Sec. 3.2, we can apply this method to estimate the number of PSR–BH systems in the Galaxy. We produce estimates using both the event- and population-based merger detection rates calculated by Abbott et al. (2021). We scale these merger detection rates reported in Abbott et al. (2021) to a range distance of 100 Mpc, which are then used as the target function in the max-

imum likelihood framework. We use the same α_{NSBH} that was derived with the assumptions in Sec. 2.

The corner plot showing the posterior distribution for $N_{\text{obs,NSBH}}$ and β_{NSBH} for the event- and population-based merger detection rates is shown in Fig. 4. The maximum likelihood values corresponding to the event-based merger detection rate are $N_{\text{obs,NSBH,e}} = 2.29 \pm 0.01$ and $\beta_{\text{NSBH,e}} = 0.0483 \pm 0.0001$, while those corresponding to the population-based merger detection rate are $N_{\text{obs,NSBH,p}} = 6.20 \pm 0.04$ and $\beta_{\text{NSBH,p}} = 0.0473 \pm 0.0003$.

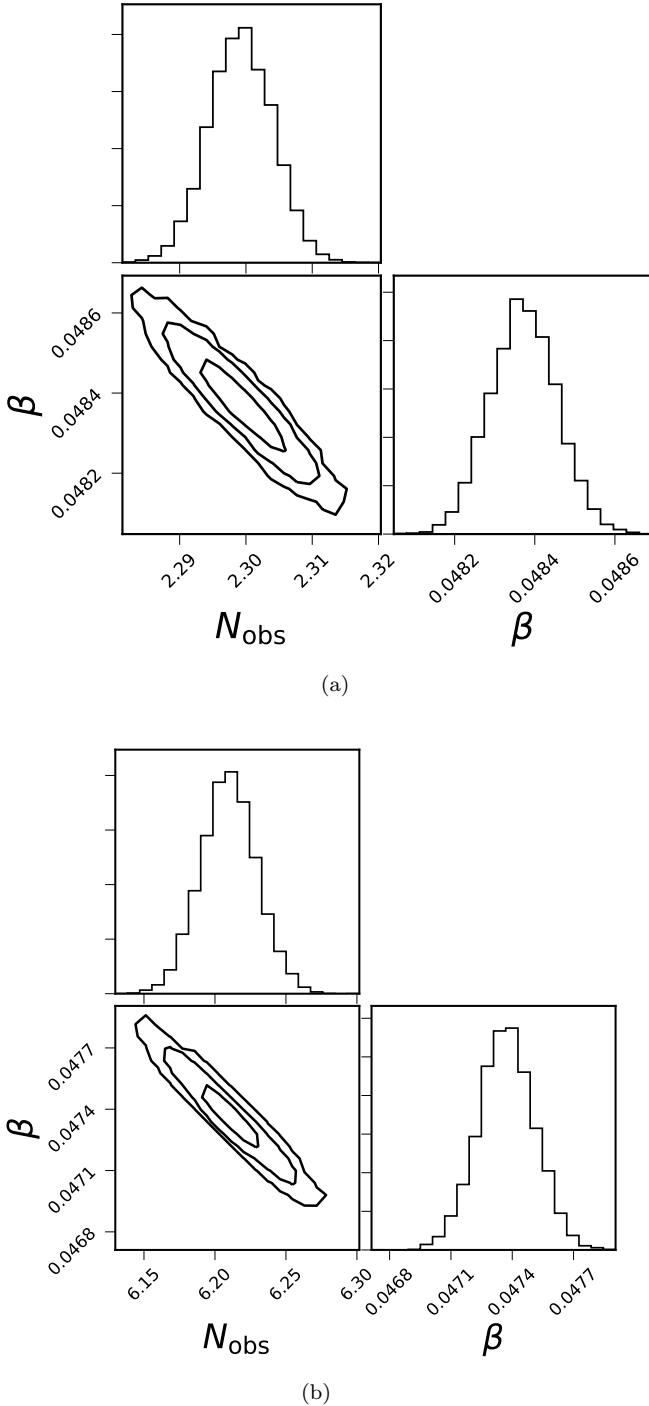


Figure 4. Results from the maximum likelihood analysis for the population of PSR–BH systems in the Galaxy. The corner plot shows the posterior distributions for the parameters in Eq. 3 for the PSR–BH systems in the Galaxy based on the event-based rate estimate (panel (a)) and population-based rate estimate (panel (b)) derived in Abbott et al. (2021). The contours represent 1-, 2-, and 3- σ credible regions.

These values of $N_{\text{obs,NSBH}}$ can be used to estimate the average number of PSR–BH systems, $\langle N_{\text{obs,NSBH}} \rangle$

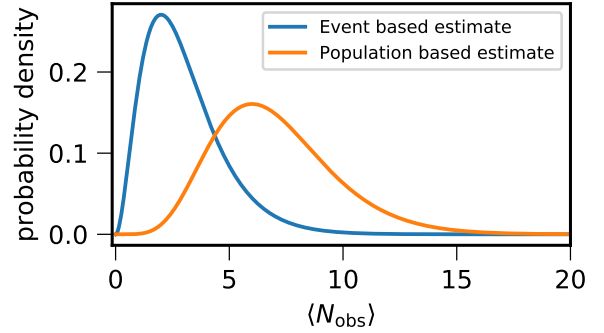


Figure 5. Distribution of the expected number of observable PSR–BH systems from the maximum likelihood analysis described in Sec. 3.1.

that might be observable given the population parameters and radio surveys that we have considered in this work (Eq. 7 in Kim et al. 2003). This distribution is shown in Fig. 5, and predicts that we should be able to detect $\langle N_{\text{obs,NSBH,e}} \rangle = 2_{-1}^{+5}$ and $\langle N_{\text{obs,NSBH,p}} \rangle = 6_{-4}^{+7}$ if the event-based and population-based merger detection rates are accurately estimated by LIGO–Virgo respectively.

The maximum likelihood value of β which encodes the average beaming correction factor and lifetimes for the PSR–BH population is larger than the corresponding value found for DNS systems in Sec. 3.2. If we assume that a plausible range for beaming correction factors for canonical pulsars is $1 \leq f_b \leq 10$ (Tauris & Manchester 1998), then we get a range of average lifetimes $20 \text{ Myr} \leq \tau_{\text{life}} \leq 220 \text{ Myr}$ for the PSR–BH systems in the Galaxy. This suggests that, similar to the DNS systems, the merger detection rate estimate might be driven by a few compact PSR–BH binary systems.

3.4. Total number of detectable PSR–BH systems

Similarly, we can also estimate the size of the total population of PSR–BH that are beaming towards the Earth (Kim et al. 2003). For the event-based merger detection rate, the size of the population is $N_{\text{tot,e}} = 77_{-53}^{+202}$, while for the population-based merger detection rate, the size of the population is $N_{\text{tot,e}} = 233_{-122}^{+272}$. Given the uncertainty on the beaming correction factor from the maximum likelihood framework, it is difficult to estimate the total population of PSR–BH systems in the Galaxy by including the systems that might not be beaming towards Earth.

As discussed in Secs. 3.2 and 3.3, a small subset of PSR–BH systems might be dominating the estimation of the merger detection rate. With the Galactic DNS population, there are twice as many DNS systems as

ones that merge within a Hubble time, which is usually adopted as the cutoff for the lifetime of systems that are included in merger rate calculations. Thus, we can expect there to be more PSR–BH systems, both observable and total, in the Galaxy than that estimated above. How many more, however, is difficult to predict since none of these systems have been found yet, and they are expected to follow a different evolutionary scenario compared to Galactic DNS systems.

4. FUTURE PROSPECTS

As we show in Sec. 2, despite the lack of a radio detected PSR–BH system, there could be as many as 150 PSR–BH systems (at the 95% credible interval) in the Galaxy that are beaming towards the Earth. On the other hand, as shown in Sec. 3, if the LIGO–Virgo derived merger detection rate estimate is accurate, then we can expect to detect as many as 7 or 13 PSR–BH systems (95% credible interval), while as many as 279 or 505 (95% credible interval) detectable PSR–BH systems are beaming towards the Earth for the event-based and population-based rate estimates respectively.

4.1. Probability of detecting a PSR–BH system

Given these estimates of the number of PSR–BH systems in the Galaxy, we can calculate the probability of detecting these systems in current radio surveys. Using the same procedure as in Pol et al. (2021), we assume that the number of PSR–BH binaries in the Milky Way that are beaming towards Earth is given by the upper limit calculated in Sec. 2.2. We choose to use this estimate so that the detection probabilities calculated here will be conservative estimates, since the detection probability is proportional to the size of the population. Next, we simulate 10^3 different realizations of this population of PSR–BH binaries using PSRPOPpy, with the same prior distributions as described in Sec. 2. We then “run” each of the surveys listed in Table 1 on each of the realizations and calculate the probability with which the PSR–BH systems are detected in any of these surveys.

The probability for detection of PSR–BH binaries for each of the current radio surveys is shown in Fig. 6. The PALFA survey has the highest probability of detecting at least one PSR–BH system, which is to be expected given the high sensitivity of the survey. This is followed by the HTRU–mid latitude, Parkes multibeam and Arecibo driftscan surveys, while the HTRU low–latitude and GBNCC surveys have the smallest probability of detecting a PSR–BH system.

4.2. Where are these PSR–BH systems?

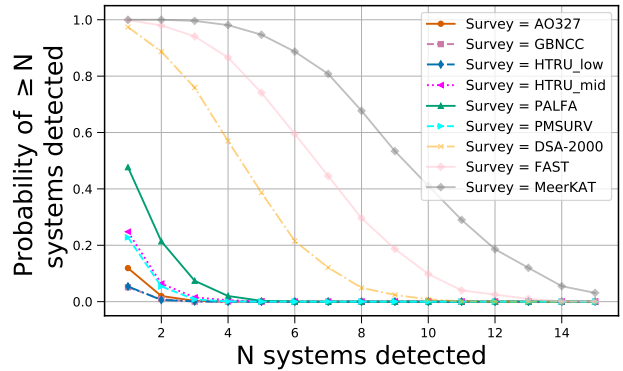


Figure 6. Probability of detecting a PSR–BH system with current and future radio surveys, assuming there are ~ 150 PSR–BH systems in the Galaxy beaming towards Earth. The PALFA survey at the Arecibo radio telescope has the highest probability of detecting a PSR–BH system of the current surveys. Surveys underway with MeerKAT and FAST and planned with DSA–2000 should almost certainly detect at least one of these systems.

Given the above probabilities, it is worth investigating why none of these systems have been detected in any radio pulsar surveys thus far.

One reason for the lack of detection of PSR–BH systems could be that these systems exist pre-dominantly as compact binaries, i.e. binaries with orbital periods \sim hours or less. There is some precedence for this assumption from ab initio stellar evolution simulations, where PSR–BH systems in wide binaries could get disrupted in either one of the supernova explosions that form the constituent objects in the binary (Giacobbo & Mapelli 2020; Podsiadlowski et al. 2004). Detection of pulsars in binaries is hampered due to the effect of the degradation of the S/N ratio induced by the orbital motion of the pulsar in the orbit around its companion (Johnston & Kulkarni 1991; Bagchi et al. 2013). The orbital degradation factor (Bagchi et al. 2013) is inversely proportional to the mass of the companion in the binary. Thus, pulsars in orbit around a black hole companion will suffer from larger degradation in their observed S/N relative to a pulsar in orbit around another neutron star, given the same orbital configuration (see for e.g., Bagchi et al. 2013). However, the degradation is weaker for pulsars with larger spin periods (i.e. canonical pulsars), and we expect these pulsars to be prevalent in PSR–BH systems. Thus, if PSR–BH systems are in compact orbits, they could be as difficult to detect as the known Galactic DNS systems. As shown in Pol et al. (2021), the probability of detecting compact or ultra-compact pulsar binaries can be increased by using smaller survey integration times.

Another hurdle towards detection of PSR–BH systems is the relatively poor timing precision shown by canonical pulsars relative to millisecond pulsars. In particular, canonical pulsars exhibit larger red noise in their residuals along with larger measurement uncertainties (Parthasarathy et al. 2019; Lower et al. 2020), which can serve to mask the signatures of the binary motion. This phenomenon will mainly affect pulsars in wider orbits around black holes (thus only weakly influencing the merger detection rate), thereby reducing sensitivity to such PSR–BH systems (Jones 2021). Note that PSR–BH systems can have, on average, orbital periods as large as ~ 10 days and still merge within a Hubble time. Detection of pulsars in such wide PSR–BH binaries will require a combination of multi-year monitoring of candidate canonical pulsars and higher sensitivity telescopes for conducting these timing observations (Jones 2021).

The position of the potential PSR–BH binaries in the Galaxy could also serve to decrease the probability of detecting these systems. In particular, if PSR–BH systems are more likely to be formed in the Galactic center (Pfahl & Loeb 2004; Chennamangalam & Lorimer 2014), then all of the current surveys will be severely hampered by the dispersion and scattering introduced by the dense interstellar medium (ISM) present towards the Galactic center. The solution to mitigate ISM effects is to conduct surveys of the Galactic center at higher radio frequencies (Macquart & Kanekar 2015), and a number of them have been carried out to date (Rajwade et al. 2017; Hyman et al. 2019; Eatough et al. 2013). However, pulsar emission tends to be weaker at higher radio frequencies (Bates et al. 2013), which combined with the orbital degradation effect can compound the difficulty in detecting PSR–BH systems in the Galactic center.

4.3. *New and future telescopes*

The advent of a new generation of radio telescopes with larger collecting areas will allow us to probe the pulsar population at lower flux densities. Among these new instruments is the Five hundred meter Aperture Spherical Telescope (FAST, Nan et al. 2011) which is a single dish telescope offering unparalleled sensitivity, while the MeerKAT radio telescope (Jonas & MeerKAT Team 2016), a pre-cursor to the Square Kilometer Array (SKA, Carilli & Rawlings 2004), and DSA-2000 (Deep Synoptic Array, Hallinan et al. 2019) are interferometric telescopes which provide large fields of view and effective collecting areas.

The pulsar survey parameters for these new instruments are listed in Table 1 and the probability of detecting a PSR–BH system is shown in Fig. 6. All of the new

surveys have significantly better sensitivity than those of the current pulsar surveys, as a result of which they are almost certain to detect at least one PSR–BH system. While the single dish configuration of FAST gives it the best sensitivity of the three new surveys, MeerKAT’s access to most of the Galactic plane (given its location in the Southern hemisphere) as well as a larger field of view than FAST results in it having a higher probability of detecting more than one PSR–BH system. Both of these radio telescopes have initiated surveys of the Galaxy to search for new binary pulsars (Han et al. 2021; Sanidas et al. 2018) and provide the best opportunity to detect any PSR–BH system that might have been too faint for the current radio telescopes and surveys. In Fig. 6, we also illustrate detection prospects for surveys planned with the DSA-2000 concept proposed to the Astro2020 Decadal Survey (Hallinan et al. 2019), and show that this telescope will be competitive with FAST and MeerKAT in searching for PSR–BH systems. Eventually the SKA will provide even better sensitivity, allowing us to probe most of the pulsar population in the Galaxy.

In addition to finding new PSR–BH systems, the higher sensitivity of these new radio telescopes also allows us to produce timing solutions with a lower root-mean-square spread (σ_{TOA}) in the residuals. This improvement in the timing accuracy is important for PSR–BH systems, since the timing accuracy determines the amount of information that can be extracted from a PSR–BH system. For example, Wex & Kopeikin (1999) showed that for young pulsars with timing precision of $\sigma_{\text{TOA}} \sim 100 \mu\text{s}$, any PSR–BH system with orbital periods less than 10 days (i.e. those that are considered in this work), will allow determining the mass of the black hole to better than 5% accuracy, while PSR–BH systems with orbital periods less than three days will allow measurements of the spin of the black hole within reasonable observing campaigns. As described in Sec. 3.4, the merger detection rate estimated using the LIGO–Virgo NS–BH mergers implies the existence of PSR–BH systems with lifetimes that are small enough to support the existence of relatively compact PSR–BH systems. A detection of one of these systems is thus guaranteed to provide an accurate estimate of the mass of the black hole, if not the spin of the black hole.

5. CONCLUSION

In this analysis, we use information from radio pulsar surveys and LIGO–Virgo NS–BH merger detections to estimate the number of PSR–BH systems in the Milky Way. We find that the non-detection of a PSR–BH system in radio pulsar surveys implies a 95% credible upper limit of ~ 150 PSR–BH systems in the Galaxy that

are beaming towards the Earth. Using a range distance of 100 Mpc, this corresponds to a 95% credible upper limit on the NS–BH merger detection rate of 7.6 yr^{-1} for LIGO–Virgo. This rate is consistent with the merger detection rates derived by LIGO–Virgo (Abbott et al. 2021), implying that a non-detection of a PSR–BH system in radio surveys so far is consistent with LIGO’s detection of two NS–BH mergers.

We also use the merger detection rates derived by LIGO–Virgo using their detection of two NS–BH systems to estimate the number of observable PSR–BH systems in the Milky Way, using which we can determine the population of PSR–BH systems that are beaming towards Earth. We find that if the LIGO–Virgo merger detection rates are accurate, there should be $\langle N_{\text{obs,NSBH,e}} \rangle = 2_{-1}^{+5}$ and $\langle N_{\text{obs,NSBH,D}} \rangle = 6_{-4}^{+7}$ detectable PSR–BH systems in the Galaxy corresponding to the event-based and population-based merger detection rates respectively (Abbott et al. 2021). This corresponds to a total of $N_{\text{tot,e}} = 77_{-53}^{+202}$ and $N_{\text{tot,e}} =$

233_{-122}^{+272} PSR–BH systems in the Galaxy that are beaming towards the Earth.

We estimate the probability of detecting these PSR–BH systems, and show that the PALFA survey at the Arecibo radio telescope has the highest probability of detecting one of these systems. We also discuss the hurdles involved in detecting PSR–BH systems with radio pulsar surveys and show how new and upcoming radio telescopes might help alleviate some of these hurdles, while also providing the necessary timing accuracy to enable accurate measurements of the mass and spin of the black hole in the PSR–BH system.

1 The authors would like to thank Megan Jones for
2 discussions on the difficulty of detecting PSR–BH sys-
3 tems in wide binaries. N.P. acknowledges support from
4 the VIDA Fellowship from the Vanderbilt Initiative
5 for Data-intensive Astrophysics. N.P. and M.A.M. are
6 members of the NANOGrav Physics Frontiers Center
7 (NSF PHY-1430284). M.A.M. and D.R.L. have addi-
8 tional support from NSF OIA-1458952.

REFERENCES

- Abbott, R., Abbott, T. D., Abraham, S., et al. 2021, *ApJL*, 915, L5, doi: [10.3847/2041-8213/ac082e](https://doi.org/10.3847/2041-8213/ac082e)
- Bagchi, M., Lorimer, D. R., & Wolfe, S. 2013, *MNRAS*, 432, 1303, doi: [10.1093/mnras/stt559](https://doi.org/10.1093/mnras/stt559)
- Bailes, M., Jameson, A., Abbate, F., et al. 2020, *PASA*, 37, e028, doi: [10.1017/pasa.2020.19](https://doi.org/10.1017/pasa.2020.19)
- Bates, S. D., Lorimer, D. R., Rane, A., & Swiggum, J. 2014, *MNRAS*, 439, 2893, doi: [10.1093/mnras/stu157](https://doi.org/10.1093/mnras/stu157)
- Bates, S. D., Lorimer, D. R., & Verbiest, J. P. W. 2013, *MNRAS*, 431, 1352, doi: [10.1093/mnras/stt257](https://doi.org/10.1093/mnras/stt257)
- Belczynski, K., Kalogera, V., & Bulik, T. 2002, *ApJ*, 572, 407, doi: [10.1086/340304](https://doi.org/10.1086/340304)
- Belczynski, K., Repetto, S., Holz, D. E., et al. 2016, *ApJ*, 819, 108, doi: [10.3847/0004-637X/819/2/108](https://doi.org/10.3847/0004-637X/819/2/108)
- Breton, R. P., Kaspi, V. M., McLaughlin, M. A., et al. 2012, *ApJ*, 747, 89, doi: [10.1088/0004-637X/747/2/89](https://doi.org/10.1088/0004-637X/747/2/89)
- Broekgaarden, F. S., Berger, E., Neijssel, C. J., et al. 2021, *arXiv e-prints*, arXiv:2103.02608. <https://arxiv.org/abs/2103.02608>
- Burgay, M., D’Amico, N., Possenti, A., et al. 2005, in *Astronomical Society of the Pacific Conference Series*, Vol. 328, Binary Radio Pulsars, ed. F. A. Rasio & I. H. Stairs, 53
- Carilli, C. L., & Rawlings, S. 2004, *NewAR*, 48, 979, doi: [10.1016/j.newar.2004.09.001](https://doi.org/10.1016/j.newar.2004.09.001)
- Chattopadhyay, D., Stevenson, S., Hurley, J. R., Bailes, M., & Broekgaarden, F. 2021, *MNRAS*, 504, 3682, doi: [10.1093/mnras/stab973](https://doi.org/10.1093/mnras/stab973)
- Chen, K., & Ruderman, M. 1993, *ApJ*, 402, 264, doi: [10.1086/172129](https://doi.org/10.1086/172129)
- Chennamangalam, J., & Lorimer, D. R. 2014, *MNRAS*, 440, L86, doi: [10.1093/mnras/flu025](https://doi.org/10.1093/mnras/flu025)
- Clausen, D., Sigurdsson, S., & Chernoff, D. F. 2013, *MNRAS*, 428, 3618, doi: [10.1093/mnras/sts295](https://doi.org/10.1093/mnras/sts295)
- Cordes, J. M., Freire, P. C. C., Lorimer, D. R., et al. 2006, *ApJ*, 637, 446, doi: [10.1086/498335](https://doi.org/10.1086/498335)
- Deneva, J. S., Stovall, K., McLaughlin, M. A., et al. 2013, *ApJ*, 775, 51, doi: [10.1088/0004-637X/775/1/51](https://doi.org/10.1088/0004-637X/775/1/51)
- Eatough, R. P., Kramer, M., Klein, B., et al. 2013, in *Neutron Stars and Pulsars: Challenges and Opportunities after 80 years*, ed. J. van Leeuwen, Vol. 291, 382–384, doi: [10.1017/S1743921312024209](https://doi.org/10.1017/S1743921312024209)
- Faucher-Giguère, C.-A., & Kaspi, V. M. 2006, *ApJ*, 643, 332, doi: [10.1086/501516](https://doi.org/10.1086/501516)
- Ferdman, R. D., Freire, P. C. C., Perera, B. B. P., et al. 2020, *Nature*, 583, 211, doi: [10.1038/s41586-020-2439-x](https://doi.org/10.1038/s41586-020-2439-x)
- Foreman-Mackey, D., Hogg, D. W., Lang, D., & Goodman, J. 2013, *PASP*, 125, 306, doi: [10.1086/670067](https://doi.org/10.1086/670067)
- Foster, R. S., Cadwell, B. J., Wolszczan, A., & Anderson, S. B. 1995, *ApJ*, 454, 826, doi: [10.1086/176535](https://doi.org/10.1086/176535)

- Giacobbo, N., & Mapelli, M. 2020, *ApJ*, 891, 141, doi: [10.3847/1538-4357/ab7335](https://doi.org/10.3847/1538-4357/ab7335)
- Grunthal, K., Kramer, M., & Desvignes, G. 2021, *MNRAS*, doi: [10.1093/mnras/stab2198](https://doi.org/10.1093/mnras/stab2198)
- Hallinan, G., Ravi, V., Weinreb, S., et al. 2019, in *Bulletin of the American Astronomical Society*, Vol. 51, 255. <https://arxiv.org/abs/1907.07648>
- Han, J. L., Wang, C., Wang, P. F., et al. 2021, *Research in Astronomy and Astrophysics*, 21, 107, doi: [10.1088/1674-4527/21/5/107](https://doi.org/10.1088/1674-4527/21/5/107)
- Hyman, S. D., Frail, D. A., Deneva, J. S., et al. 2019, *ApJ*, 876, 20, doi: [10.3847/1538-4357/ab11c8](https://doi.org/10.3847/1538-4357/ab11c8)
- Johnston, H. M., & Kulkarni, S. R. 1991, *ApJ*, 368, 504, doi: [10.1086/169715](https://doi.org/10.1086/169715)
- Jonas, J., & MeerKAT Team. 2016, in *MeerKAT Science: On the Pathway to the SKA*, 1
- Jones, M. L. 2021, in prep
- Keith, M. J., Jameson, A., van Straten, W., et al. 2010, *MNRAS*, 409, 619, doi: [10.1111/j.1365-2966.2010.17325.x](https://doi.org/10.1111/j.1365-2966.2010.17325.x)
- Kim, C., Kalogera, V., & Lorimer, D. R. 2003, *ApJ*, 584, 985, doi: [10.1086/345740](https://doi.org/10.1086/345740)
- Kopparapu, R. K., Hanna, C., Kalogera, V., et al. 2008, *The Astrophysical Journal*, 675, 1459. <http://stacks.iop.org/0004-637X/675/i=2/a=1459>
- Kramer, M., & Wex, N. 2009, *Classical and Quantum Gravity*, 26, 073001, doi: [10.1088/0264-9381/26/7/073001](https://doi.org/10.1088/0264-9381/26/7/073001)
- Kramer, M., Stairs, I. H., Manchester, R. N., et al. 2006, *Science*, 314, 97, doi: [10.1126/science.1132305](https://doi.org/10.1126/science.1132305)
- Kruckow, M. U., Tauris, T. M., Langer, N., Kramer, M., & Izzard, R. G. 2018, *MNRAS*, 481, 1908, doi: [10.1093/mnras/sty2190](https://doi.org/10.1093/mnras/sty2190)
- Lazarus, P., Brazier, A., Hessels, J. W. T., et al. 2015, *ApJ*, 812, 81, doi: [10.1088/0004-637X/812/1/81](https://doi.org/10.1088/0004-637X/812/1/81)
- Liu, K., Eatough, R. P., Wex, N., & Kramer, M. 2014, *MNRAS*, 445, 3115, doi: [10.1093/mnras/stu1913](https://doi.org/10.1093/mnras/stu1913)
- Lomiashvili, D., & Lyutikov, M. 2014, *MNRAS*, 441, 690, doi: [10.1093/mnras/stu564](https://doi.org/10.1093/mnras/stu564)
- Lorimer, D. R. 2005, *Living Reviews in Relativity*, 8, 7, doi: [10.12942/lrr-2005-7](https://doi.org/10.12942/lrr-2005-7)
- Lorimer, D. R., Faulkner, A. J., Lyne, A. G., et al. 2006, *MNRAS*, 372, 777, doi: [10.1111/j.1365-2966.2006.10887.x](https://doi.org/10.1111/j.1365-2966.2006.10887.x)
- Lower, M. E., Bailes, M., Shannon, R. M., et al. 2020, *MNRAS*, 494, 228, doi: [10.1093/mnras/staa615](https://doi.org/10.1093/mnras/staa615)
- Lyne, A. G., Burgay, M., Kramer, M., et al. 2004, *Science*, 303, 1153, doi: [10.1126/science.1094645](https://doi.org/10.1126/science.1094645)
- Macquart, J.-P., & Kanekar, N. 2015, *ApJ*, 805, 172, doi: [10.1088/0004-637X/805/2/172](https://doi.org/10.1088/0004-637X/805/2/172)
- Manchester, R. N., Hobbs, G. B., Teoh, A., & Hobbs, M. 2005, *AJ*, 129, 1993, doi: [10.1086/428488](https://doi.org/10.1086/428488)
- Manchester, R. N., Lyne, A. G., Camilo, F., et al. 2001, *MNRAS*, 328, 17, doi: [10.1046/j.1365-8711.2001.04751.x](https://doi.org/10.1046/j.1365-8711.2001.04751.x)
- McKernan, B., Ford, K. E. S., & O'Shaughnessy, R. 2020, *MNRAS*, 498, 4088, doi: [10.1093/mnras/staa2681](https://doi.org/10.1093/mnras/staa2681)
- Moré, J. J. 1978, *The Levenberg-Marquardt algorithm: Implementation and theory*, Vol. 630, 105–116, doi: [10.1007/BFb0067700](https://doi.org/10.1007/BFb0067700)
- Nan, R., Li, D., Jin, C., et al. 2011, *International Journal of Modern Physics D*, 20, 989, doi: [10.1142/S0218271811019335](https://doi.org/10.1142/S0218271811019335)
- Newville, M., Otten, R., Nelson, A., et al. 2021, *lmfit/lmfit-py* 1.0.2, 1.0.2, Zenodo, doi: [10.5281/zenodo.4516651](https://doi.org/10.5281/zenodo.4516651)
- Özel, F., & Freire, P. 2016, *ARA&A*, 54, 401, doi: [10.1146/annurev-astro-081915-023322](https://doi.org/10.1146/annurev-astro-081915-023322)
- Pan, Z., Qian, L., Ma, X., et al. 2021, *ApJL*, 915, L28, doi: [10.3847/2041-8213/ac0bbd](https://doi.org/10.3847/2041-8213/ac0bbd)
- Parthasarathy, A., Shannon, R. M., Johnston, S., et al. 2019, *MNRAS*, 489, 3810, doi: [10.1093/mnras/stz2383](https://doi.org/10.1093/mnras/stz2383)
- Pfahl, E., & Loeb, A. 2004, *ApJ*, 615, 253, doi: [10.1086/423975](https://doi.org/10.1086/423975)
- Podsiadlowski, P., Langer, N., Poelarends, A. J. T., et al. 2004, *ApJ*, 612, 1044, doi: [10.1086/421713](https://doi.org/10.1086/421713)
- Pol, N., McLaughlin, M., & Lorimer, D. R. 2019, *ApJ*, 870, 71, doi: [10.3847/1538-4357/aaf006](https://doi.org/10.3847/1538-4357/aaf006)
- Pol, N., McLaughlin, M., Lorimer, D. R., & Garver-Daniels, N. 2021, *ApJ*, 912, 22, doi: [10.3847/1538-4357/abe9b7](https://doi.org/10.3847/1538-4357/abe9b7)
- Portegies Zwart, S. F., & McMillan, S. L. W. 2000, *ApJL*, 528, L17, doi: [10.1086/312422](https://doi.org/10.1086/312422)
- Rajwade, K. M., Lorimer, D. R., & Anderson, L. D. 2017, *MNRAS*, 471, 730, doi: [10.1093/mnras/stx1661](https://doi.org/10.1093/mnras/stx1661)
- Ransom, S. M., Stairs, I. H., Archibald, A. M., et al. 2014, *Nature*, 505, 520, doi: [10.1038/nature12917](https://doi.org/10.1038/nature12917)
- Ridolfi, A., Gautam, T., Freire, P. C. C., et al. 2021, *MNRAS*, 504, 1407, doi: [10.1093/mnras/stab790](https://doi.org/10.1093/mnras/stab790)
- Sanidas, S., Caleb, M., Driessen, L., et al. 2018, in *Pulsar Astrophysics the Next Fifty Years*, ed. P. Weltevrede, B. B. P. Perera, L. L. Preston, & S. Sanidas, Vol. 337, 406–407, doi: [10.1017/S1743921317009310](https://doi.org/10.1017/S1743921317009310)
- Santoliquido, F., Mapelli, M., Bouffanais, Y., et al. 2020, *ApJ*, 898, 152, doi: [10.3847/1538-4357/ab9b78](https://doi.org/10.3847/1538-4357/ab9b78)
- Stairs, I. H. 2004, *Science*, 304, 547, doi: [10.1126/science.1096986](https://doi.org/10.1126/science.1096986)
- Stovall, K., Lynch, R. S., Ransom, S. M., et al. 2014, *ApJ*, 791, 67, doi: [10.1088/0004-637X/791/1/67](https://doi.org/10.1088/0004-637X/791/1/67)
- Tan, C. M., Bassa, C. G., Cooper, S., et al. 2018, *ApJ*, 866, 54, doi: [10.3847/1538-4357/aade88](https://doi.org/10.3847/1538-4357/aade88)
- Tauris, T. M., & Manchester, R. N. 1998, *Monthly Notices of the Royal Astronomical Society*, 298, 625, doi: [10.1046/j.1365-8711.1998.01369.x](https://doi.org/10.1046/j.1365-8711.1998.01369.x)

Urquhart, R., Bahramian, A., Strader, J., et al. 2020, ApJ, 904, 147, doi: [10.3847/1538-4357/abb6fc](https://doi.org/10.3847/1538-4357/abb6fc)

Wex, N., & Kopeikin, S. M. 1999, ApJ, 514, 388, doi: [10.1086/306933](https://doi.org/10.1086/306933)

Wex, N., Liu, K., Eatough, R. P., et al. 2013, in Neutron Stars and Pulsars: Challenges and Opportunities after 80 years, ed. J. van Leeuwen, Vol. 291, 171–176, doi: [10.1017/S1743921312023538](https://doi.org/10.1017/S1743921312023538)

Ye, C. S., Fong, W.-f., Kremer, K., et al. 2020, ApJL, 888, L10, doi: [10.3847/2041-8213/ab5dc5](https://doi.org/10.3847/2041-8213/ab5dc5)

Zhang, B. 2003, Acta Astronomica Sinica, 44, 215. <https://arxiv.org/abs/astro-ph/0209160>

Zhang, B., Harding, A. K., & Muslimov, A. G. 2000, ApJL, 531, L135, doi: [10.1086/312542](https://doi.org/10.1086/312542)